Liquid-Gas Dynamic System under Vibration

Timothy J. O'Hern, John R. Torczynski, and Jonathan R. Clausen*

Engineering Sciences Center; Sandia National Laboratories; PO Box 5800; Albuquerque, New Mexico 87185-0840 USA
tjohern@sandia.gov, jrtorcz@sandia.gov, jclause@sandia.gov

Abstract

A small amount of gas can change the dynamics of a liquid-filled spring-mass-damper system under vibration. A spring-supported piston that fits closely within a liquid-filled housing is considered. A post fixed to the housing protrudes partway into a hole through the piston, so the damping from forcing liquid through this narrow gap is large and depends on the piston position. When gas is absent, the piston's vibrational response is highly overdamped. When a small amount of gas is added, Bjerknes forces cause some of the gas to migrate below the piston. The resulting gas regions above and below the piston form a pneumatic spring that enables the liquid to move with the piston so that very little liquid is forced through the gap. This "Couette mode" has low damping and thus has a strong resonance near the frequency given by the pneumatic spring constant and the piston mass. At this frequency, the piston motion is large, and the nonlinearity from the piston-position-dependent damping produces a net force on the piston. This "rectified" force can be many times the piston's weight and can cause the piston to compress its supporting spring. Theoretical models, numerical simulations, and experiments with bellows as surrogate gas regions are used to investigate the dynamics of this system. Theory and simulations are in good agreement, but experiments show systematic differences due to additional damping on the piston.

Keywords: Vibration, liquid, gas, bellows, spring, piston, damping, rectification

1. Introduction

The motion of a piston within a vibrated liquid-filled cylindrical housing can be dramatically changed by introducing a small amount of gas [1,2,3,4]. Fig. 1 shows photographs of this situation with vibration off and on, and Fig. 2 shows a schematic of its cross section in the left diagram. The piston is supported against gravity by a coiled-wire spring. A post fixed to the housing protrudes partway into a circular hole along the piston's axis, so the flow resistance of the gap between the piston and the post varies with the piston's vertical position. This inner gap and the outer gap between the piston and the housing are both narrow, so any piston motion forcing liquid through these gaps is highly damped [5]. When the housing is vibrated vertically, the piston moves downward against its supporting coiled-wire spring under certain conditions [1,2,3,4]. Prior to this downward piston motion, some of the gas from above the piston migrates down below the piston and becomes trapped below the piston by Bjerknes forces [6,7].

Herein, we use theory, simulations, and experiments to investigate how gas regions above and below the piston can cause the piston to move downward during vertical vibration and how the piston and post geometry affect this rectified motion. In this study, we do not investigate how the lower gas region is formed but instead focus on the dynamic effect of these two gas regions once they exist. Following the pioneering study of Bjerknes [6], many researchers have studied the downward rectified motion of a gas bubble in a vibrated liquid. Most studies have focused on a small isolated spherical bubble in a large open geometry, with relatively few studies focusing on the formation and stability of a lower gas region in a highly confined geometry of the type in Fig. 1 and Fig. 2. An extensive bibliography for downward rectified bubble motion is given elsewhere [7].

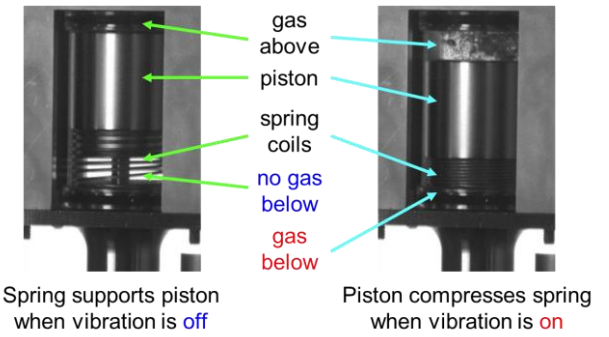

Figure 1. Photographs of piston in transparent housing. Vertical vibration causes piston in liquid-filled housing with gas present to move down against its supporting spring [1,2,3].

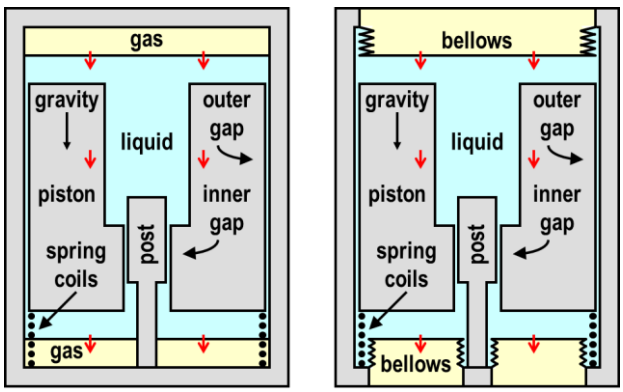

Figure 2. Schematic cross sections of systems considered [3,4]. Length of inner gap depends linearly on piston position. Compressible regions are gas (left) or bellows (right). Arrows represent velocity vectors for Couette mode.

* Sandia National Laboratories is a multi-program laboratory managed and operated by Sandia Corporation, a wholly owned subsidiary of Lockheed Martin Corporation, for the U.S. Department of Energy's National Nuclear Security Administration under contract DE-AC04-94AL85000. This manuscript has been authored by Sandia Corporation under Contract No. DE-AC04-94AL85000 with the U.S. Department of Energy. The United States Government retains and the publisher, by accepting the article for publication, acknowledges that the United States Government retains a non-exclusive, paid-up, irrevocable, world-wide license to publish or reproduce the published form of this manuscript, or allow others to do so, for United States Government purposes.

In this paper, we analyze the dynamic effect of these gas regions by studying the surrogate system in the right diagram in Fig. 2. In this system, two bellows with similar pressure-volume relationships replace the corresponding two gas regions. Thus, the effect of the pneumatic spring formed by these compressible regions (gas or bellows) can be analyzed by itself without the additional complexity of gas migration. Compressible regions both above and below the piston are essential since a single compressible region in an incompressible liquid cannot produce a pneumatic spring. In this study, the geometry is axisymmetric, and the piston moves only in the vertical direction. The latter assumption is justified since the outer gap is extremely narrow relative to the piston diameter for realistic situations [4,5].

Other researchers have reported similar phenomena but have not performed rigorous analyses of these systems. More than 50 years ago, Clark, McClamroch, and Walker observed a piston move down against its supporting coiled-wire spring in a vibrated liquid-filled housing with gas present [8,9]. However, they neither analyzed their results nor published them in the archival literature. More than 30 years ago, Chelomey briefly described experiments in which vibration caused a large heavy sphere fitting closely within a liquid-filled tube to rise to the free surface when air was present [10]. However, he did not analyze this situation but instead just presented it as one of several "paradoxes" (his term) in vibration mechanics.

We organize the remainder of this paper as follows. First, we review the theory for the surrogate piston-bellows system. Second, we present numerical simulations of the piston-bellows system and compare theoretical and simulation results. Third, we present experimental results for the piston-bellows system and compare them to theoretical results. Fourth, we summarize the implications of our work for future research in this area.

2. Theoretical Analysis

The physical mechanism leading to vibration-induced net (rectified) piston motion is as follows [1,2,3,4]. When a small amount of gas is present, Bjerknes forces [6] cause some of the gas to migrate below the piston. The resulting pneumatic spring enables the liquid to move with the piston so that no extra liquid is forced through the gaps. This "Couette mode" [3,4] has low damping and a strong resonance near the frequency given by the pneumatic spring constant and the total piston and liquid mass. Near resonance, the piston motion is large, and the nonlinearity from the piston-position-dependent damping produces a net force on the piston. This net (rectified) force can be many times the piston's weight and can cause the piston to compress its supporting spring, as observed in the experiments [1,2,3].

Recently, Romero and co-workers [4] developed a theory for rectified piston motion in this system. The piston and the bellows obey Newton's 2nd Law, and the liquid obeys the unsteady incompressible Navier-Stokes equations. Quasi-steady liquid flow in the gap-dominated regime is considered, so the liquid forces on the piston and the bellows are sums of damping terms (damping coefficients multiplied by object velocities) and mass terms (added masses multiplied by object accelerations). They derive ordinary differential equations for the piston and bellows displacements leading to expressions for the oscillatory and net (rectified) piston displacements caused by the oscillating acceleration. They observe that the slight departure of the piston-bellows motion from the pure Couette mode is responsible for the rectified motion of the piston.

Two area ratios appear in their analysis, as in Fig 2 [3,4]. The quantity κ is the ratio of the cross sectional areas A_{BU} and A_{BL} of the upper and lower bellows (and, for an incompressible liquid, is also the ratio of the lower to upper bellows velocities):

$$\kappa = A_{BU}/A_{BL} \to 1 \text{ in this study.} \tag{1}$$

Herein, this quantity is set equal to unity (equal-area bellows), so the upper and lower bellows ends move at the same velocity. The quantity λ is a ratio involving three cross sectional areas, where the upper bellows has area A_B, the piston has area A_P, and the outer and inner gaps have total area A_G:

$$\lambda = \frac{A_B}{A_P + (A_G/2)}. \tag{2}$$

When the ratio of the piston and upper-bellows velocities equals this value, the Couette mode is achieved, and no extra liquid is forced through the gaps, so damping is small. Fig. 2 shows this situation for both the piston-gas and piston-bellows systems.

Their resulting system of ordinary differential equations represents a nonlinear damped-harmonic-oscillator equation for the displacements Z_P and Z_B of the piston and the upper bellows from their equilibrium positions [3,4]:

$$\frac{d}{dt}\left(\left(\tilde{\mathbf{M}}+\mathbf{M}\right)\frac{d\mathbf{Z}}{dt}\right)+\mathbf{B}\frac{d\mathbf{Z}}{dt}+\tilde{\mathbf{K}}\mathbf{Z}=\mathbf{F},\ \mathbf{Z}=\begin{pmatrix}Z_P\\Z_B\end{pmatrix}; \tag{3}$$

$$\tilde{\mathbf{M}}=\begin{pmatrix}M_P & 0\\0 & M_B\end{pmatrix},\ \tilde{\mathbf{K}}=\begin{pmatrix}K_P & 0\\0 & K_B\end{pmatrix}; \tag{4}$$

$$\mathbf{M}=\left(M_{ij}\right),\ \mathbf{B}=\left(B_{ij}\right),\ \{i,j\}\in\{1,2\}; \tag{5}$$

$$\mathbf{F}=-\begin{pmatrix}M_P-M_{LP}\\M_W+M_V\end{pmatrix}g_1\sin[\omega t],\ \omega=2\pi f; \tag{6}$$

$$K_B=K_{BU}+\kappa^2K_{BL},\ M_B=M_{BU}+\kappa^2M_{BL},\ M_W=\rho L_BA_B,$$
$$M_V=M_{BU}+\kappa M_{BL},\ M_P=\rho_PV_P,\ M_{LP}=\rho V_P; \tag{7}$$

$$M_{ij}=\rho\int_V\tilde{\mathbf{u}}_i\cdot\tilde{\mathbf{u}}_j dV,\ B_{ij}=2\mu\int_V\tilde{\mathbf{S}}_i:\tilde{\mathbf{S}}_j dV; \tag{8}$$

$$\tilde{\mathbf{S}}_i=\frac{1}{2}\left(\frac{\partial\tilde{\mathbf{u}}_i}{\partial\mathbf{x}}+\frac{\partial\tilde{\mathbf{u}}_i}{\partial\mathbf{x}}^T\right),\ \tilde{\mathbf{u}}=\frac{\mathbf{u}}{U}. \tag{9}$$

Here, $\tilde{\mathbf{M}}$, $\mathbf{M}$, $\mathbf{B}$, and $\tilde{\mathbf{K}}$ are the actual-mass, added-mass, damping, and stiffness matrices, and $\mathbf{F}$ and $\mathbf{Z}$ are the force and displacement vectors. The masses M_P, M_{LP}, M_W, M_V, M_B, M_{BU}, and M_{BL} represent the piston, its displaced liquid, the liquid between the upper and lower bellows, a bellows term, the total bellows, and the upper and lower bellows. The spring constants K_P, K_B, K_{BU}, and K_{BL} represent the piston, the total bellows, and the upper and lower bellows. The oscillating acceleration $g_1\sin[\omega t]$ has amplitude g_1, angular frequency $\omega=2\pi f$, and frequency f. The entries M_{ij} and B_{ij} of $\mathbf{M}$ and $\mathbf{B}$ are found from steady-Stokes mobility solutions $\mathbf{u}_i$ when only object i is moving and it has velocity $U\hat{\mathbf{e}}_z$ [3,4].

The strong near-linear dependence of the damping matrix $\mathbf{B}$ on the piston position Z_P is the key nonlinearity that yields a nonzero net force on the piston during vibration. Although the added-mass matrix $\mathbf{M}$ has the same type of nonlinearity, its term is integrable and thus does not contribute to the net force. The main contributions to the piston rectified force F_{rect} and the piston rectified velocity U_{rect} are expressed in terms of the solution $\mathbf{Z}$ to the linearized version of Eq. (3) [3,4]:

$$F_{\text{rect}}=\lambda\frac{\partial B_{11}}{\partial Z_P}\left\langle Z_P\frac{dZ_B}{dt}\right\rangle,\ U_{\text{rect}}=\frac{F_{\text{rect}}}{B_{11}}. \tag{10}$$

3. Numerical Simulations

Numerical simulations of the piston-bellows system are performed and compared to the theory in the previous section. The key parameters and their nominal values are given below.

f	acceleration frequency	50 Hz
f_0	Couette-mode frequency	107 Hz
g_0	steady gravitational acceleration	9.81 m/s^2
g_1	acceleration amplitude	20 g_0
K_B	bellows spring constant (total)	14,126 N/m
K_P	piston spring constant	26 N/m
L_B	distance between bellows ends	75.8952 mm
L_I	maximum length of inner gap	5.0800 mm
L_O	length of outer gap	23.6220 mm
M_B	bellows mass (total)	0 kg
M_P	piston mass	0.0742 kg
R_B	bellows radius (here, both)	8.3820 mm
R_{I1}	post radius, inner gap	2.4384 mm
R_{I2}	piston radius, inner gap	2.5400 mm
R_{O1}	piston radius, outer gap	11.3792 mm
R_{O2}	housing radius, outer gap	11.4300 mm
κ	upper-to-lower bellows area ratio	1
λ	bellows-piston-gap area ratio	0.5672
μ	liquid viscosity (20-cSt PDMS)	0.019 Pa·s
	liquid viscosity (10-cSt PDMS)	0.000935 Pa·s
ρ	liquid density (20-cSt PDMS)	950 kg/m^3
	liquid density (10-cSt PDMS)	935 kg/m^3
ρ_P	piston density (stainless steel)	8000 kg/m^3
ω	angular frequency ($2\pi f$)	100π rad/s

Fig. 3 shows the axisymmetric computational domain used. At equilibrium, the piston is positioned so that the inner gap has half its maximum length. As discussed above, the piston and both bellows obey Newton's 2nd Law, and the liquid obeys the unsteady incompressible Navier-Stokes equations.

Two types of simulations are performed for this situation. First, COMSOL Multiphysics [11] is used to perform steady Stokes mobility simulations to find the entries for the damping and added-mass matrices $\mathbf{B}$ and $\mathbf{M}$, as discussed above [3,4]:

$$\mathbf{M} = \begin{pmatrix} 0.413702 & -0.237824 \\ -0.237824 & 0.144245 \end{pmatrix} \text{ kg}, \tag{11}$$

$$\mathbf{B} = \begin{pmatrix} 0.558909 & -0.316958 \\ -0.316958 & 0.179762 \end{pmatrix} \times 10^4 \text{ kg/s}; \tag{12}$$

$$\frac{\partial \mathbf{M}}{\partial Z_P} = \begin{pmatrix} 0.634948 & -0.360472 \\ -0.360472 & 0.204442 \end{pmatrix} \times 10^2 \text{ kg/m}, \tag{13}$$

$$\frac{\partial \mathbf{B}}{\partial Z_P} = \begin{pmatrix} 0.193943 & -0.110010 \\ -0.110010 & 0.062402 \end{pmatrix} \times 10^7 \text{ kg/s}. \tag{14}$$

The vector $\mathbf{\Lambda}$ representing the Couette mode is almost a null vector for the matrices $\mathbf{B}$ and $\mathbf{M}$, so this vector yields the Couette-mode resonant frequency f_0 [3,4]:

$$\mathbf{\Lambda} = \begin{pmatrix} \lambda \\ 1 \end{pmatrix}, \quad f_0 = \frac{1}{2\pi} \sqrt{\frac{\mathbf{\Lambda}^T \tilde{\mathbf{K}} \mathbf{\Lambda}}{\mathbf{\Lambda}^T (\tilde{\mathbf{M}} + \mathbf{M}) \mathbf{\Lambda}}}. \tag{15}$$

For these conditions, the resonant frequency is $f_0 = 107$ Hz.

Second, unsteady Arbitrary Lagrangian Eulerian (ALE) simulations are performed in which the piston, the two bellows, and the liquid move due to the oscillating acceleration. Sandia's finite-element code ARIA [12] is used for these simulations. The ALE method is extended by using a sliding-mesh algorithm to account for the large piston displacements [13]. In this algorithm, a portion of the mesh moves with the piston, and the remainder of the mesh is fixed to the post. These two mesh sections are nonconformal along a line bisecting the inner gap, with the piston mesh sliding along the post mesh. Extensive tests have confirmed the accuracy of this approach [13].

Fig. 4 shows the piston displacements from simulation and theory for the 20-cSt liquid with a frequency of $f = 50$ Hz and an acceleration amplitude of $g_1 = 20 g_0$ over a 1-s interval. The initial piston position is as in Fig. 3. After a transient, the simulation yields an oscillation plus a steady downward drift. The oscillation amplitude and the steady downward drift from the theory are in good agreement with the simulation results. Although the frequency $f = 50$ Hz is well below the resonant frequency of $f_0 = 107$ Hz, the piston moves downward by 6% of the inner-gap length of 5.0800 mm in just 1 s.

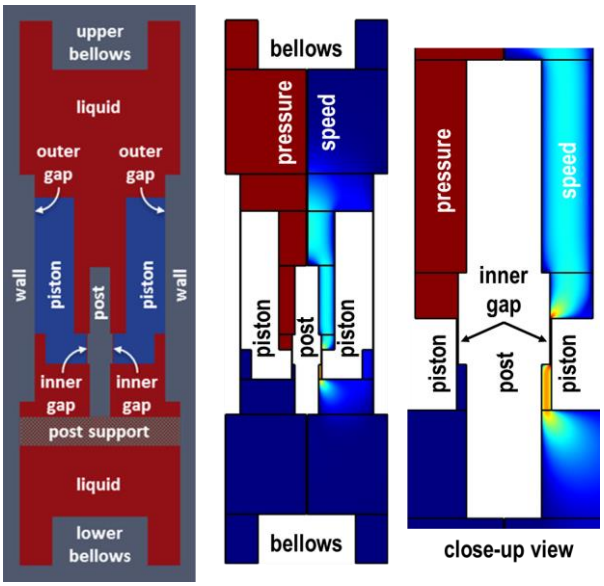

Figure 3. Left: axisymmetric computational domain. Right pair: one of two steady-Stokes solutions used to compute $\mathbf{B}$ and $\mathbf{M}$. Inner-gap protrusions are initially half-aligned.

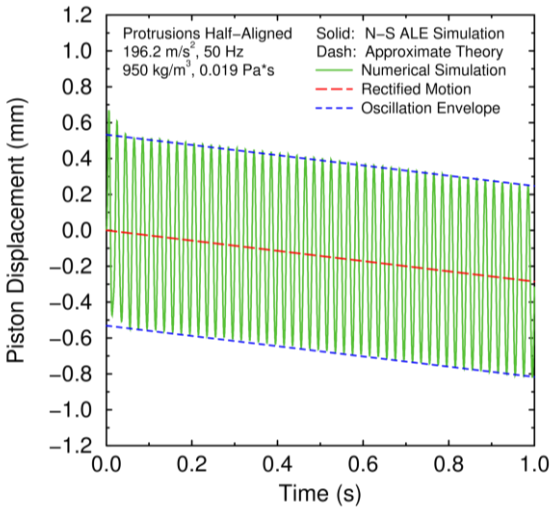

Figure 4. Piston displacement from theory and simulation. Green solid curve from simulation has oscillation and drift. Blue and red theory curves are from Eq. (3) and Eq. (10).

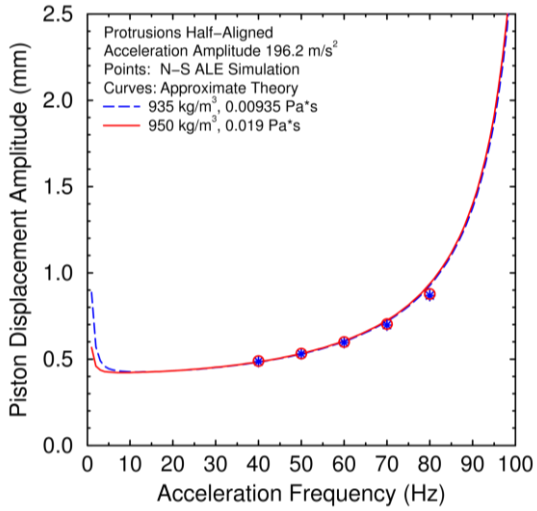

Figure 5. Piston displacement amplitude at fixed acceleration amplitude versus frequency for both liquids from theory and simulations (resonance is at 107 Hz).

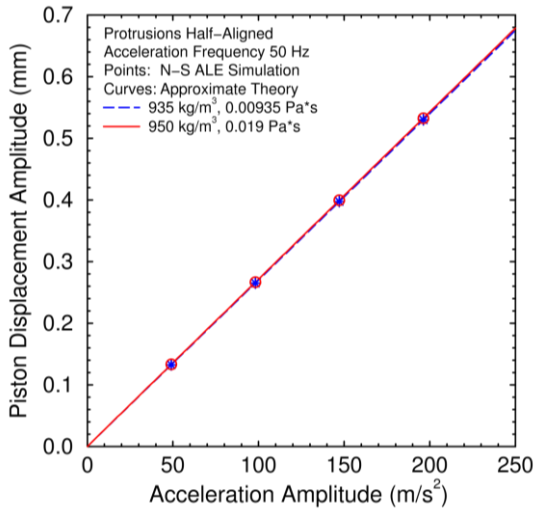

Figure 6. Piston displacement amplitude at fixed frequency versus acceleration amplitude for both liquids from theory and simulations.

Figs. 5-8 show results from a parameter study in which the acceleration frequency f and the acceleration amplitude g_1 are varied about the nominal values. In these plots, theoretical results are shown using curves, and numerical results are shown using symbols. Two sets of values are used for liquid properties: $\rho = 935$ kg/m^3, $\mu = 0.00935$ Pa·s (10 cSt PDMS) and also $\rho = 950$ kg/m^3, $\mu = 0.019$ Pa·s (20 cSt PDMS). In these plots, the 10-cSt and 20-cSt results are shown in blue and red, respectively.

Figs. 5-6 show the piston displacement amplitude for the sinusoidal part of its motion, as in Fig. 4. The displacement amplitude is nearly independent of the liquid, is almost linear in the acceleration amplitude (exactly for the theory), and grows strongly as the resonance frequency of 107 Hz is approached. Theory and simulation are in good agreement although a slight divergence is seen as the resonance frequency is approached. This divergence is attributed to large piston displacements near resonance, for which the accuracy of the theory decreases [3,4].

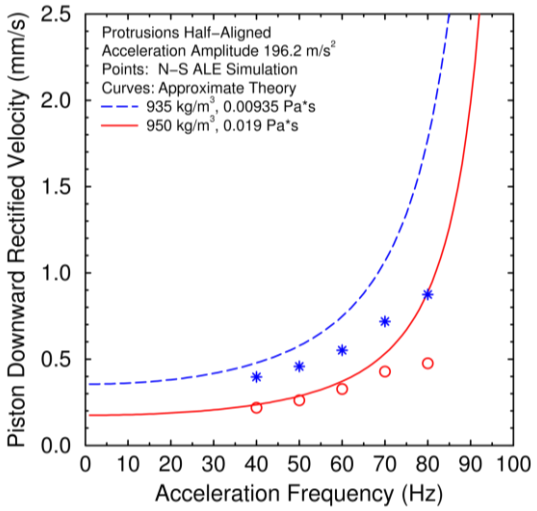

Figure 7. Piston downward rectified velocity at fixed acceleration amplitude versus frequency for both liquids from theory and simulations (resonance is at 107 Hz).

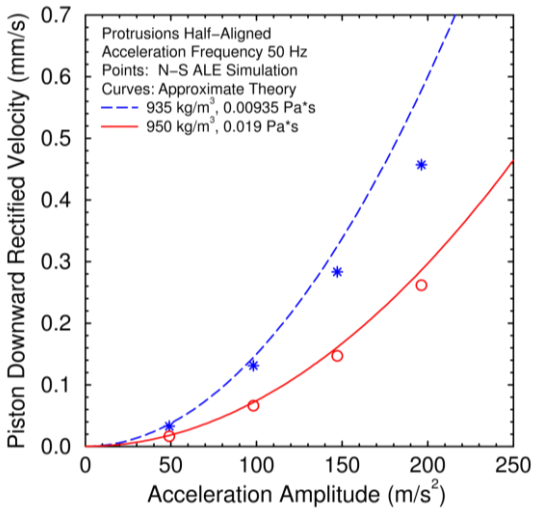

Figure 8. Piston downward rectified velocity at fixed frequency versus acceleration amplitude for both liquids from theory and simulations.

Figs. 7-8 show the piston rectified velocity, which is the net part of its motion, as in Fig. 4 (here, positive downward). The rectified velocity varies nearly inversely with the liquid viscosity, is almost quadratic in the acceleration amplitude (exactly for the theory), and grows strongly as the resonance is approached. The theoretical values are always greater than the numerical values, and this overprediction increases as the resonance frequency is approached and/or the acceleration amplitude is increased. Moreover, the overprediction increases as the liquid viscosity is decreased. This overprediction is again attributed to large piston displacements near resonance, for which the accuracy of the theory decreases [3,4].

Thus, the theory slightly overpredicts the piston downward rectified velocity and, by inference, the downward rectified force on the piston. Nevertheless, due to its ease of evaluation relative to the intensity of numerical simulations, the theory is a useful tool for interpreting the experimental results presented in the following section.

4. Experiments

The experimental test cell has an internal geometry similar to the right schematic in Fig. 2. A transparent acrylic housing contains a 22.8600-mm-ID cylindrical cavity, which in turn contains a movable 22.7584-mm-OD stainless steel piston, a post fixed to the cylinder bottom, and a coiled-wire spring that supports the piston above the cylinder bottom. The spring initially presses the piston against stops just below the top end of the cylinder. The piston and the post have protrusions that create the variable-length inner gap, as in Figs. 2-3. The internal volume is completely filled with silicone oil: all air is removed.

Two compressible bellows are attached to the test cell. Servometer Model FC-13 electroformed bellows [14], with a 16.7640-mm mean diameter and a pressure-volume relationship similar to that of a 1.5 mL bubble, are used. These bellows are welded to base plates that are attached to the top and bottom ends of the test cell. The bellows spring constants and damping characteristics are measured with a commercial texture tester and by mounting them on the shaker and finding their resonant frequencies for different attached masses. Their spring constants are in reasonable agreement with nominal values [14].

The test cell is mounted on a shaker and subjected to vertical vibration. A Labworks Model ET-140 electrodynamic shaker and a PCB Piezoelectronics uniaxial accelerometer are used. A LabVIEW program controls the shaker and records accelerometer output and other data. The vibration control parameters are the frequency f and the displacement amplitude z_1, which set the acceleration amplitude $g_1 = z_1\omega^2$, where $\omega = 2\pi f$ is the angular frequency.

These parameters are varied to determine the conditions under which downward piston rectified motion occurs. Experiments are performed for frequencies of $f = 50\text{-}300$ Hz, displacement amplitudes of $z_1 = 0.004\text{-}1.5$ mm, which jointly yield acceleration amplitudes of $g_1 = 3\text{-}30g_0 = 29.4\text{-}294$ m/s^2. Clearco polydimethylsiloxane (PDMS) silicone oils with kinematic viscosities of 10 cSt and 20 cSt are used [15]. All experiments are performed at room temperature and pressure.

Piston-position histories are measured using an Allied Vision Technologies Manta GigE camera with a LabVIEW edge-tracking routine. Images are recorded using a Phantom v9.1 high-speed camera, typically run at 1000 frames/second. The test cell is backlit with a diffuse LED array light source.

Most experiments are run in a semi-automated fashion. Increasing and decreasing sine sweeps over $f = 50\text{-}200$ Hz with a fixed acceleration amplitude g_1 are run over 300 s. Subsequently, the next value of the acceleration amplitude g_1 is selected, and the sweep process is repeated. The piston position is continuously recorded throughout each sweep. However, at certain frequencies, the vibration synchronizes with the camera frame rate, and the motion is not measured accurately, so the data at these frequencies are deleted during post-processing.

Figs. 9-10 show results from increasing-frequency sweeps that progress from smaller to larger acceleration amplitudes. The piston starts in the "up" position at the top of the cylinder, where it is held against the stops by its supporting spring. If the acceleration amplitude is large enough, the piston undergoes downward rectified motion at some frequency. The piston then stays in the "down" position at the bottom of the cylinder over some range of frequency. When some yet higher frequency is reached, the piston returns to the top of the cylinder. The "piston-down" frequency range is bounded by the lower and higher frequencies at which the piston position changes. This range decreases as the acceleration amplitude is decreased and vanishes when the acceleration amplitude becomes low enough (for $g_1 < 10g_0$ in Fig. 9).

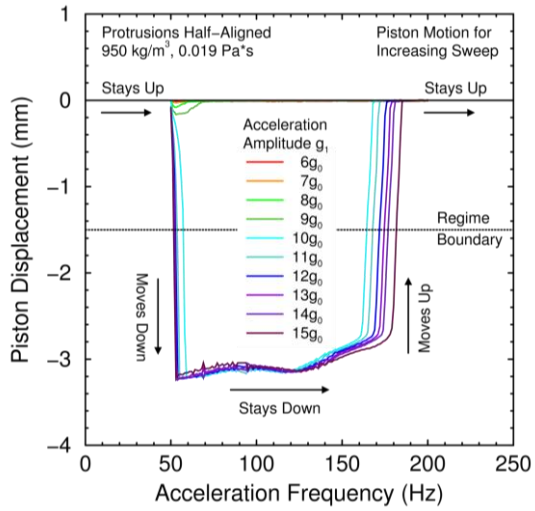

Figure 9. Piston-displacement data from increasing sine sweeps of frequency at different fixed acceleration amplitudes.

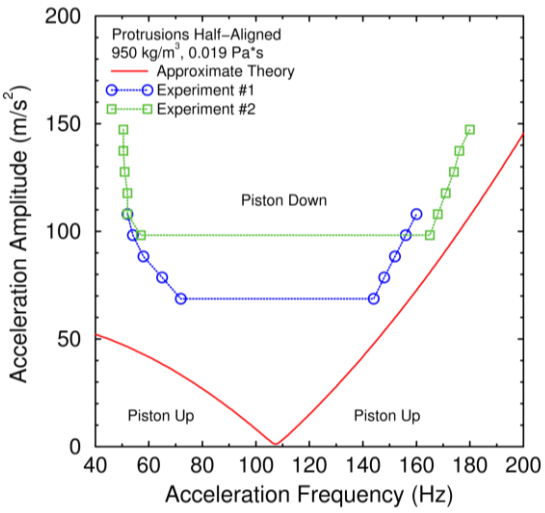

Figure 10. Regime map from increasing sine sweeps at fixed acceleration. Piston starts up, then goes down at some frequency, and then goes back up at a higher frequency.

Fig. 10 shows a regime map constructed from data like in Fig. 9. The frequencies at the "up-down" and "down-up" transitions of piston positon are plotted at the acceleration amplitude used. Two identical experiments produce somewhat different piston-down regimes. Although their left and right regime boundaries are similar, their "floors" below which the piston stays up differ significantly. The corresponding theoretical regime boundary, on which the downward rectified force on the piston equals the upward net force from the spring, gravity, and buoyancy, is also plotted. Unlike the experimental regime boundary, the theoretical regime boundary has no floor although the acceleration amplitude becomes small at the resonant frequency of 107 Hz.

The reasons for the significant variation in the floor of the experimental regime boundary and for the difference between the experimental and theoretical regime boundaries have not yet been determined. It is conjectured that additional damping from the squeeze-film force on the piston when it is pressed against the stops may cause the experimental acceleration amplitudes to be larger than the theoretical values and to be more variable.

5. Conclusions

Theory, simulations, and experiments have been used to characterize the dynamic response of a spring-mass-damper system during vibration. In this system, a piston moves within a liquid-filled cylinder with compressible regions (gas or bellows) at the top and the bottom. A spring supports the piston, all gaps are narrow, and the gap between the post and the hole through the piston depends on the piston position. Thus, the damping associated with forcing liquid through this gap varies almost linearly with the piston position within the housing.

Adding a small amount of gas can change the vibration dynamics of this liquid-filled piston-gas system. Bjerknes forces cause some gas to migrate below the piston, and the resulting pneumatic spring enables the liquid to move with the piston so that no extra liquid is forced through the gaps. This "Couette mode" has low damping and a strong resonance near the frequency given by the pneumatic spring constant and the piston and liquid mass. The response is large near this frequency, and the nonlinearity from the varying gap length produces a net force on the piston. This rectified (net) force causes the piston to move down and compress its supporting spring.

A recently developed theory for the surrogate piston-bellows system is compared to finite element simulations using an ALE method with a sliding-mesh technique that limits mesh distortion. The theory and simulation results are in good agreement for the oscillation amplitude of the piston and in fair agreement for the rectified (net) downward drift of the piston. The differences become larger as the liquid viscosity is reduced and/or the resonance frequency is approached. This behavior is reasonable because the piston motion is large in these situations, whereas the theory is developed under the assumption that the piston motion is small.

Experiments are performed to determine the vibration conditions under which the surrogate piston-bellows system exhibits downward rectified motion of the piston. Increasing sweeps of frequency with fixed acceleration amplitude show one of two characteristic behaviors. Either the piston remains up over the entire frequency range examined, or the piston goes down at some frequency and goes back up at a larger frequency. These transition frequencies and acceleration amplitudes define regime boundaries in the map of the system's dynamics. Generally speaking, the piston goes down for large acceleration amplitudes with medium frequencies but stays up for either large or small frequencies with modest acceleration amplitudes.

The theory is used to construct a regime map by equating the downward rectified force to the net upward force from the spring, gravity, and buoyancy. This force balance yields the two transition frequencies for a given acceleration amplitude. Like the experimental regime map, the theoretical regime map indicates that the piston stays up at low frequencies, stays down at medium frequencies, and stays up for large frequencies. A further similarity is that the frequency range over which the piston stays down becomes larger as the acceleration amplitude is increased. A difference is that the theoretical regime map does not possess a "floor", a value of the acceleration amplitude below which the piston always stays up.

Future work will focus on three areas. First, more complete data sets will be acquired for more extensive model validation. Second, the role of the stops against which the piston is pressed by its spring will be investigated. Third, the division of gas between the upper and lower regions will be studied because this division determines the strength of the pneumatic spring.

Acknowledgments

The authors gratefully acknowledge technical interactions with Gilbert L. Benavides, of Sandia National Laboratories, and Louis A. Romero, formerly of Sandia National Laboratories. The authors also thank Robert M. Garcia of Sandia National Laboratories and Nialah J. Wilson of Howard University for performing some sine sweeps and measuring bellows response and Paul A. Farias of Sandia National Laboratories for designing and fabricating some of the experimental apparatus.

References

[1] Torczynski, J. R., Romero, L. A., Clausen, J. R., and O'Hern, T. J., 2014, "Vibration-induced rectified motion of a piston in a liquid-filled cylinder with bellows to mimic gas regions," *Bulletin of the American Physical Society*, **59**(20), 494.

[2] Torczynski, J. R., O'Hern, T. J., and Clausen, J. R., 2015, "Adding some gas can completely change how an object in a liquid-filled housing responds to vibration," *Bulletin of the American Physical Society*, **60**(21), 554.

[3] O'Hern, T. J., Torczynski, J. R., and Clausen, J. R., 2016, "Multiphase Effects in Dynamic Systems under Vibration," HTFEICNMM2016-1074, American Society of Mechanical Engineers, New York, NY.

[4] Romero, L. A., Torczynski, J. R., Clausen, J. R., O'Hern, T. J., and Benavides, G. L., 2016, "Gas-enabled resonance and rectified motion of a piston in a vibrated housing filled with a viscous liquid," *Journal of Fluids Engineering*, **138**(6), 061302, 1-19.

[5] Asami, T., Honda, I., and Ueyama, A., 2014, "Numerical analysis of the internal flow in an annular flow channel type oil damper," *Journal of Fluids Engineering*, **136**(3), 031101, 1-8.

[6] Bjerknes, V. F. K., 1906, *Fields of Force*, Columbia University Press, New York, NY.

[7] Romero, L. A., Torczynski, J. R., and von Winckel, G., 2014, "Terminal velocity of a bubble in a vertically vibrated liquid," *Physics of Fluids*, **26**(5), 053301, 1-32.

[8] Clark, L. G., McClamroch, N. H., and Walker, J. A., 1964, *Piston and Cylinder Vibration Study*, Report JMH/1332-4, University of Texas, Austin, TX.

[9] McClamroch, N. H., 1965, *Motion of a Gas Bubble Submerged in a Vibrating Liquid*, M.S. Thesis, University of Texas, Austin, TX.

[10] Chelomey, V. N., 1984, "Paradoxes in mechanics caused by vibrations," *Acta Astronautica*, **11**(5), 269-273.

[11] COMSOL, 2008, *COMSOL Multiphysics User's Guide*, Version 3.5a, COMSOL AB, Stockholm, Sweden.

[12] Notz, P. K., Subia, S. R., Hopkins, M. M., Moffatt, H. K., and Noble, D. R., 2007, *Aria 1.5: User Manual*, Report SAND2007-2734, Sandia National Laboratories, Albuquerque, NM.

[13] Clausen, J. R., Torczynski, J. R., Romero, L. A., and O'Hern, T. J., 2014, "Simulating rectified motion of a piston in a housing subjected to vibrational acceleration," *Bulletin of the American Physical Society*, **59**(20), 494.

[14] Servometer, 2015, Servometer Precision Manufacturing Group, Cedar Grove, NJ, http://www.servometer.com.

[15] Clearco, 2016, Clearco Products, Willow Grove, PA, "Polydimethylsiloxane," http://www.clearcoproducts.com.